

SEISMIC BEHAVIOR OF COMPOSITE EW ECS EXTERIOR BEAM-COLUMN JOINTS

Kimreth MEAS^{*1}, FAUZAN^{*2}, Tomoya MATSUI^{*3} and Hiroshi KURAMOTO^{*4}

ABSTRACT

This paper presents the results of an experimental study on two Engineering Wood Encased Concrete-Steel (EW ECS) exterior beam-column joints under varying axial load and lateral load reversals. The parameter investigated was the types of failure mode; beam flexural failure and joint shear failure. The results indicated that EW ECS exterior beam-column joints had a stable hysteresis response. In addition, excellent damage control performance was observed for the joint with beam flexural failure due to the higher uplift displacement occurred at the woody shell connection between column and beam.

Keywords: composite structures, beam-column joints, woody shell, seismic loading test

1. INTRODUCTION

Engineering Wood Encased Concrete-Steel (EW ECS) structural system as a new type of hybrid structural system has been developed to solve a problem for the limitation of story number for wooden structures that is limited to not more than three stories based on the Building Standard Law of Japan. The structure consists of EW ECS columns and Engineering Wood Encased Steel (EW ES) beams, as shown in Fig. 1. In this structure, the engineering wood used was glue laminated wood.

For the first stage of the research program, experimental and analytical studies on EW ECS columns had been conducted in last four years to investigate the seismic performances of the columns [1-3]. The results indicated that EW ECS columns had excellent hysteretic behavior and damage limit in which the presence of woody shell in the columns contributed to flexural capacity by around 12 % in maximum [1].

In the second stage, beam-column joints for EW ECS structural system (EW ECS beam-column joints) have been investigated. In these joints, the beam consists of only steel and woody shell, while the column consists of Concrete Encased Steel (CES) core with an exterior woody shell, as shown in Fig. 2.

In previous study, EW ECS interior beam-column joints had been investigated with

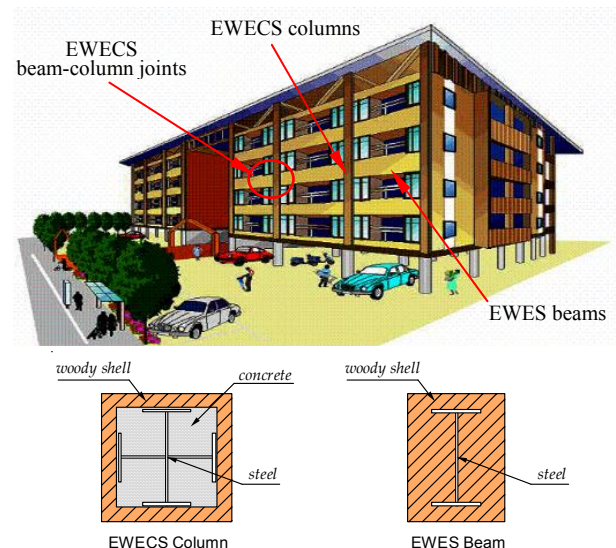


Fig. 1 Schematic view of EW ECS structures

different types of failure mode [4]. The results indicated that the interior beam-column joints had excellent seismic performance and damage limit. Furthermore, a study on EW ECS exterior beam-column joints was carried out to investigate its seismic performance.

This paper presents the results of an experimental study on seismic behavior of EW ECS exterior beam-column joints subjected to varying axial load and lateral load reversals. The types of failure mode; namely beam flexural failure and joint shear failure, were selected as the primary experimental variables in this study.

*1 Graduate Student, Dept. of Arch. & Civil Eng., Toyohashi Univ. of Technology, JCI Member

*2 Graduate Student, Dept. of Arch. & Civil Eng., Toyohashi Univ. of Technology, MSc.E., JCI Member

*3 Research Associate, Dept. of Arch. & Civil Eng., Toyohashi Univ. of Technology, Dr.E., JCI Member

*4 Associate Prof., Dept. of Arch. & Civil Eng., Toyohashi Univ. of Technology, Dr.E., JCI Member

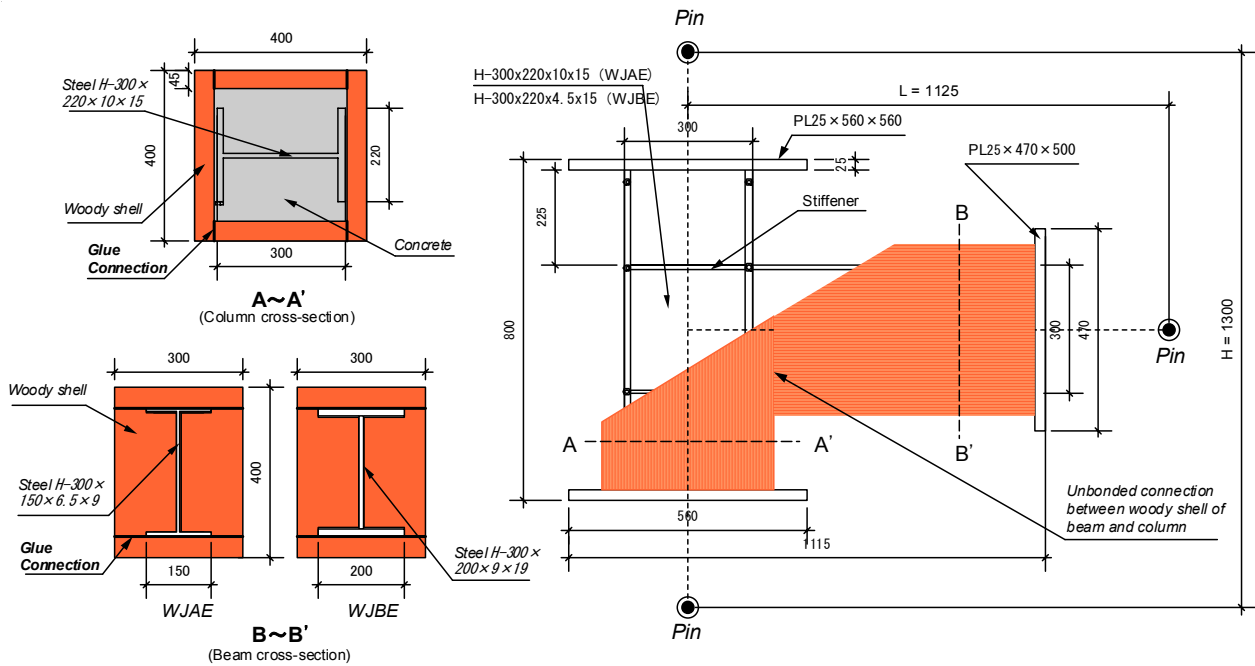


Fig. 2 Test specimen

2. EXPERIMENTAL PROGRAMS

2.1 Specimens and Materials Used

A total of two beam-column joint specimens of about one-third scale were prepared and tested, which simulated exterior beam-column joint for EWCS structural systems. One specimen was designed to have a beam flexural failure (WJAE) and the other was designed to have a joint shear failure (WJBE). The dimensions and details of the specimens are shown in Fig. 2 and Table 1.

Both specimens had a column with 1,300 mm height and 400 mm square section, and beam with 1,125 mm length (from pin to centre of the joint panel) and 300 x 400 mm section. The steel encased in each column had a single H-section steel of 300x220x10x15 mm and the thickness of the woody shell for the columns was 45 mm. Normal concrete of 28 N/mm² was used for columns of both specimens.

The main difference between these two specimens was the encased steel in the beam and joint panel, as shown in Fig. 2 and Table 1. For Specimen WJAE designed for beam flexural failure, the steels encased in the beam and panel were H-300x150x6.5x9 and H-300x220x10x15, respectively, while for Specimen WJBE designed for joint shear failure, the steels encased in the beam and panel were H-300x200x9x19 and H-300x220x4.5x15, respectively. In both specimens, the woody shell covered the H-section steel of the beams using wood glue. The mechanical properties of the steel and the woody

Table 1 Test program

Specimen		WJAE	WJBE
Type of Failure		Beam flexural failure	Joint shear failure
Woody shell Thickness of column (mm)		45	
Concrete Strength of column core (MPa)		28	
Steel on panel zone (mm)		H-300 x 220 x 10 x 15	H-300 x 220 x 4.5 x 15
Column	Built-in steel (mm)	H-300 x 220 x 10 x 15	
	Column Height: h (mm)	1300	
	Cross section : b x D (mm)	400 x 400	
Beam	Built-in steel (mm)	H-300 x 150 x 6.5 x 9	H-300 x 200 x 9 x 19
	Beam Length: h (mm)	1125	
	Cross section : b x D (mm)	300 x 400	
Applied Varying Axial Comp.		0.1No ± 3Q	

No = the total axial compressive strength of the column CES core (concrete + steel)
Q = Applied shear force

Table 2 Mechanical properties of steel

Steel	Yield Stress σ_y (MPa)	Max. Stress σ_u (MPa)	Specimen	Notes
H-300x220x10x15	304.2	447.9	Both specimens	Column flange
	318.9	460.7		Column web
PL-4.5	306.9	439.4	WJBE	Panel zone web
H-300x150x6.5x9	304.0	433.7	WJAE	Beam flange
	348.4	453.4		Beam web
H-300x200x9x19	281.1	432.9	WJBE	Beam flange
	304.3	446.2		Beam web

Table 3 Mechanical properties of woody shell

Wood type	Comp. strength parallel to grain (MPa)	Comp. strength perpendicular to grain (MPa)	Elastic Modulus Ew (GPa)
Glue laminated pine wood	51	5	11.6

Table 5 Calculated strengths

Specimen	Beam (kN)	Column (kN)	Panel (kN)
WJA	212	1220	430
WJB	346	1220	297

Table 4 Mix proportions and mechanical properties of concrete

W/C (%)	S/(S+G) (%)	Slump (cm)	Unit weight (kg/m ³)					Comp. Strength fc' (N/mm ²)
			Water (W)	Cement (C)	Sand (S)	Gravel (G)	Admixture (A)	
57	48	18.6	181	318	856	989	3.18	28

shell are listed in Tables 2 and 3, respectively. The mix proportions and properties of the concrete are given in Table 4.

The calculation results for the strength of columns, beams and joint panels of the specimens are listed in Table 5. All strengths in the table are expressed as those converted into the column shear. The ultimate strengths of the columns and beams were calculated by using flexural analysis with the superposition method [5]. The strengths of the joint panels were calculated by modifying the shear design equation of AIJ standard [5]. In the calculations, it was assumed that all materials contributed its maximum compressive strength. In addition, no tensile force in the woody shell of beam was assumed due to the unbonded connection between woody shells of the column and beam (see Fig. 2).

2.2 Test Setup and Loading Procedures

The specimen was supported by pins in both the top and bottom of the column and the end of the beam to simulate an exterior beam-column joint in a frame, in which the beam and column had inflection points in the mid-span and mid-height, respectively, as shown in Fig. 3. The specimens were loaded lateral cyclic shear forces by a horizontal hydraulic jack at the top of the column while a varying axial load was applied by two vertical hydraulic jacks. The magnitude of applied varying axial load was $N = 0.1N_o \pm 3Q$, where N_o = total axial compressive strength of steel and concrete in CES core column (5411 kN) and Q = applied shear force. The reaction stringer absorbed the shear forces in the beam caused by the load applied at the top of the column.

The incremental loading cycles were controlled by story drift angles, R , defined as the ratio of relatively vertical displacement measured by vertical transducers installed to a gauge holder at the end of the beam, to the beam length, δ/L . The lateral load sequence consisted of two cycles

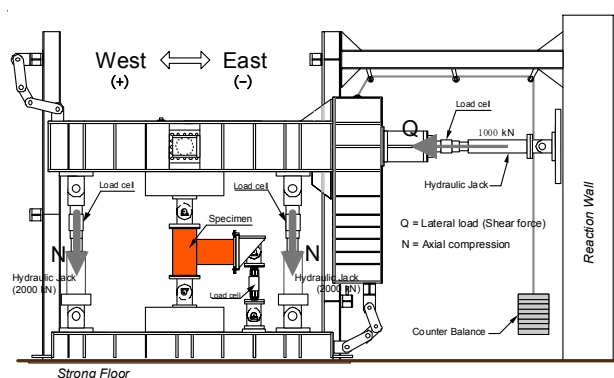


Fig. 3 Schematic view of test setup

to each story drift angle, R of 0.005, 0.01, 0.015, 0.02, 0.03 and 0.04 rad., followed by a half cycle to R of 0.05 rad.

Displacement transducers were used to measure joint distortion and deformation of beam, column and panel zone. Strains in the steel flanges and webs of the beam, column and joint panel were measured by linear and rosette strain gauges.

3. TEST RESULTS AND DISCUSSIONS

3.1 Hysteresis Characteristics and Failure Modes

The story shear versus story drift angle responses of both specimens are given in Fig. 4. In these figures, the vertical axes express the applied column shears converted from beam shears measured at the beam ends (story shear), and the horizontal axes show the story drift angle, R . The yield and maximum strengths and the corresponding story drift angles for each specimen are listed in Table 6.

As shown in Fig. 4, both specimens showed a stable shear versus story drift angle response. In Specimen WJAE with beam flexural failure, the first yielding occurred on steel flange of the beam when the applied load was -131.5 kN at R of -0.005 rad in negative cycle. There was almost no crack occurred in this specimen. However a relatively large uplift was observed at the

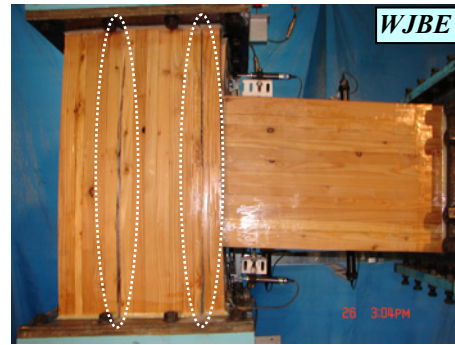
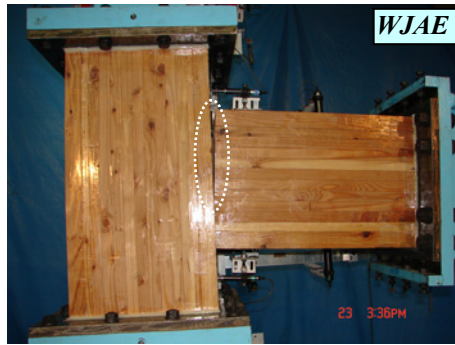


Photo 1 Crack modes of specimens at R = 0.05 rad. after loading

connection between woody shell of the beam and column as shown in Photo 1. Although the uplift increased at the joint, the shear force slightly increased until maximum capacity of 247.5 kN was reached at last story drift, R of 0.05 rad. The increase of this strength might be due to the strain hardening of the steel beam and a little contribution of woody shell of the beam in resisting load in compression zone. The specimen showed stable spindle-shaped hysteresis loop without degradation of load-carrying capacity until R of 0.05 rad. due to the formation of plastic hinge in the beam resulting in more ductile behavior.

For Specimen WJBE with joint shear failure, the first yielding occurred on steel flange of the beam at shear force of 179.3 kN at R of 0.0043 rad. The first crack of woody shell occurred at R of 0.015 rad. in the East side of the column, near the joint panel. Subsequently, the cracks extended and many other cracks occurred in the North side of the column at R of 0.02 rad. The hysteresis curve showed a little pinching-shaped but stable behavior with strength degradation after attaining the maximum capacity of 342.5 kN at R of 0.02 rad., and retaining more than 75 % of its peak strength at the last story drift angle, R of 0.05 rad. The strength degradation of the specimen might be due to the softening of concrete core and cracks in the column woody shell, caused by the repeated loadings. The maximum capacity of this specimen was higher than that of Specimen WJAE.

Different crack patterns were observed for both specimens. Compared to Specimen WJAE, more damage of the woody shell on the column faces were observed in Specimen WJBE, as shown in Photo 1. Almost no crack was observed on the woody shell of Specimen WJAE up to R of 0.05 rad. However, sink and uplift occurred at the connection between woody shell of the beam and column. For Specimen WJBE, the splitting cracks of woody shell were observed significantly on the column face. In addition, it was observed for this specimen that only slight damage occurred on woody shell of the beam.

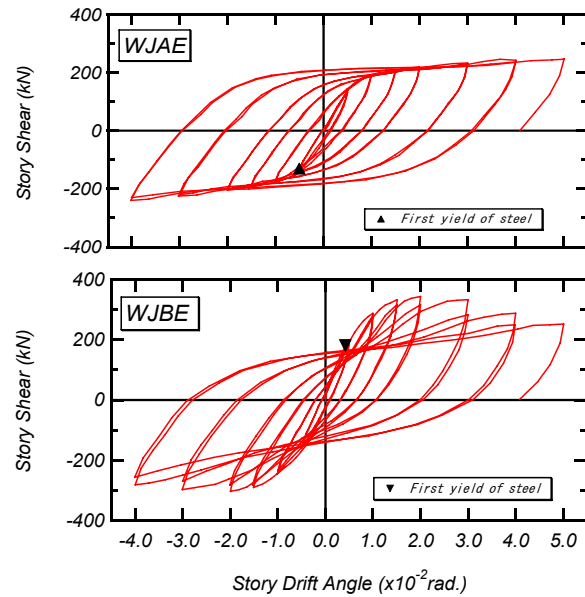


Fig. 4 Shear force - story drift relationships

Table 6 Measured strength

Specimen	at Yielding			at the Max. Capacity	
	Qy (kN)	Ry (rad.)	Location	Qmax (kN)	Rmax (rad.)
WJAE	-131.5	-0.005	Beam flange	247.5	0.05
WJBE	179.5	0.0043	Beam flange	342.5	0.02

3.2 Shear Versus Joint Distortion Response

Figure 5 shows the story shear force versus joint distortion responses for both specimens until story drift angle, R of 0.02 rad. The joint distortion, γ_p , on the horizontal axes was calculated using Eqs. 1 and 2. Fig. 6 shows the definition to calculate the joint distortion.

$$\gamma_p = \alpha_1 + \alpha_2 = \frac{\sqrt{h_p^2 + l_p^2}}{h_p \cdot l_p} \bar{x} \quad (1)$$

$$\bar{x} = \frac{\delta_1 + \delta_1' + \delta_2 + \delta_2'}{2} \quad (2)$$

where h_p , l_p and δ_1 , δ_1' , δ_2 , δ_2' are shown in Fig. 6.

As shown in Fig. 5, the spindle-shaped hysteresis curve was observed in Specimen WJAE, while Specimen WJBE showed a little pinching-shaped one. From this figure, it can also be seen the different story shear force and joint distortion values of both specimens. In Specimen WJAE, the maximum story shear was about 220 kN with the maximum joint distortion, γ_p of about 0.0015 rad., while in Specimen WJBE, the maximum story shear was about 342.5 kN, which is about 36 % higher than that of Specimen WJAE, and the maximum γ_p was 0.017 rad. The much higher joint distortion in Specimen WJBE might be due to the significant shear yielding in the panel zone.

3.3 Deformation Contributions of Each Component

Figure 7 shows the contributions of deformation by the column, beam, and joint panel to the total deformation of the joints until R of 0.02 rad. The values were obtained by measuring the deformations of beam, column and panel zone from transducers installed on the steels of each component. The deformations of the column and the joint panel were converted into the deformation of beam, as described in Fig. 8. It is clearly seen from Fig. 7 that the beam contributed the largest deformation for Specimen WJAE, while in Specimen WJBE the largest deformation was contributed by the joint panel, which was in good agreement with the types of failure mode for both specimens.

In Specimen WJAE, the contributions of deformation of column, beam and joint panel at R of 0.005 rad. were 15%, 74% and 11% respectively. At R of 0.02 rad., the panel zone and column contributions decreased slightly, while the contribution of the beam increased to around 90 %. For Specimen WJBE, the contributions of deformation of the column, beam and joint panel at R of 0.005 rad. were 12%, 41% and 47%, respectively. Due to the yield of the panel zone, the deformations of the panel increased significantly until R of 0.02 rad. At this stage, the panel contribution increased to about 60 % rad. of the total deformation of the joint, while the contribution of beam decreased.

3.4 Ultimate Strength

Figure 9 shows the calculated maximum strengths of the column, beam and joint panel in N-Q interaction diagram, which were compared with the test results. As mentioned earlier, the superposition method was used to calculate the maximum strengths of the column and beam,

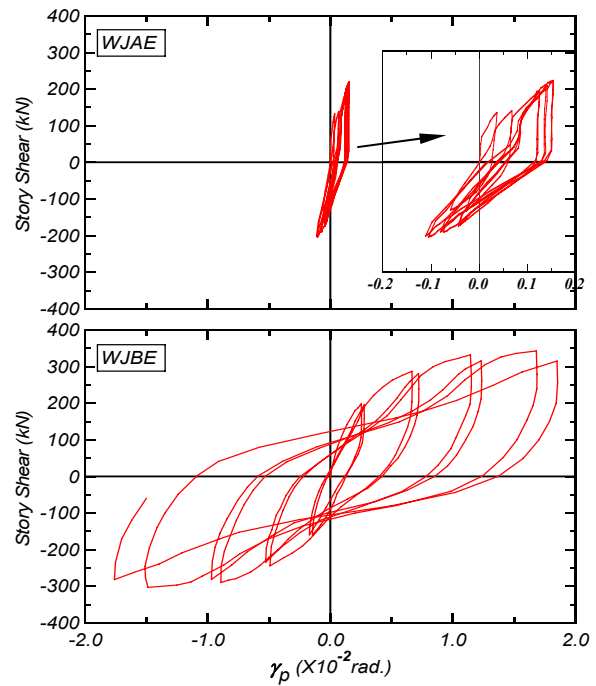


Fig. 5 Joint distortion

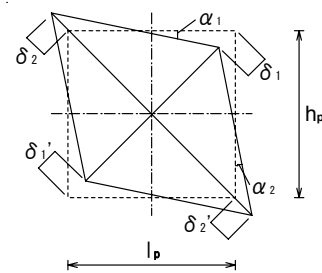


Fig. 6 Definition of joint distortion measurement

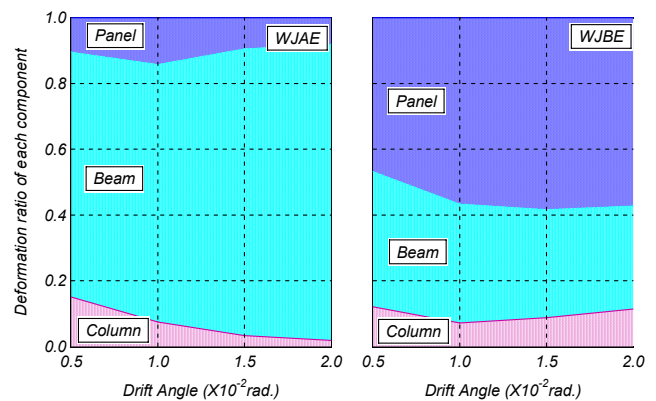


Fig. 7 Deformation ratio of each component

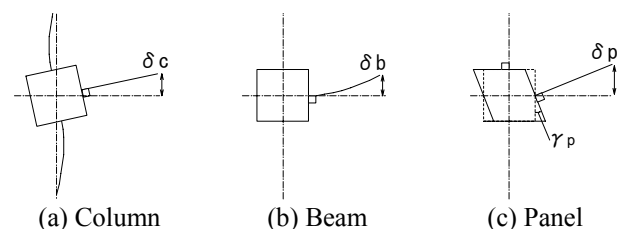


Fig. 8 Definition of deformations of each component

respectively, while the joint panel strength was calculated by modifying the AIJ standard for structural calculation of SRC structures 2001 [5] using Eqs. 3 and 4.

$$Q_{c,cal} = \frac{j_b \cdot l}{l' \cdot h - j_b \cdot l} \cdot p Q_{c,cal} \quad (3)$$

$$p Q_{c,cal} = 0.2 \cdot F_c \cdot c A_e + \frac{1.2 \cdot s \sigma_y \cdot s A}{\sqrt{3}} \quad (4)$$

where

$p Q_{c,cal}$: Calculated joint panel strength

$Q_{c,cal}$: Converting of calculated joint strength to column shear

F_c : Compressive strength of concrete

$c A_e$: Effective area of concrete cross-section in the joint panel (depth of column in joint panel \times average of column width and beam width)

$s \sigma_y$: Yield stress of steel

$s A$: Steel cross-sectional area in the joint panel

Based on the SRC standard, the effective area of concrete cross-section in the joint panel ($c A_e$) is $300 \times 350 \text{ mm}^2$, but in EWECs beam-column joints, it was assumed that $c A_e$ was $300 \times 300 \text{ mm}^2$, which is corresponding to the area of the concrete core section in the joint panel. This assumption may be conservative because the woody shell may have little contribution to the strength of the joint panel.

From Fig. 9, it can be seen that the calculated strengths had a satisfactory agreement with the measured strengths. In Specimen WJAE with beam flexural failure, the measured strength agreed with the calculated strength of the beam, while the calculated joint panel strength was higher than the measured strength. This indicated that the yielding of the beam first occurred before yielding of the panel zone.

For Specimen WJBE with joint shear failure, the calculated strength of the joint panel was slightly less than the measured strength and agreed with the calculated strength of the beam. These good comparative results indicated that the calculation method can be used to predict the ultimate strength of EWECs beam-column joints.

4. CONCLUSIONS

Based on the experimental study on EWECs exterior beam-column joints presented here, the following conclusions can be drawn:

1. EWECs exterior beam-column joints had good structural performance with a stable hysteretic behavior.
2. Both the exterior beam-column joints; with

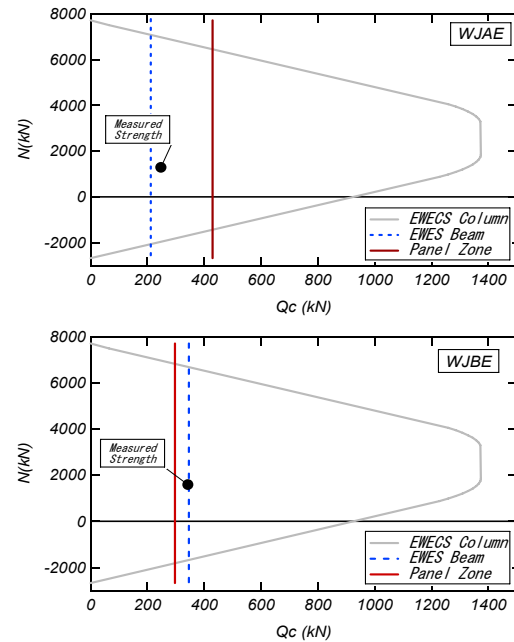


Fig. 9 Calculated strengths of column, beam and joint panel

beam flexural failure and joint shear failure, had little damage on woody shell of beam due to sink and uplift of the woody shell that occurred at the connection between woody shells of beam and column.

3. The joint distortion of specimen with joint shear failure was about ten times higher than that of the specimen with beam flexural failure due to the significant failure of the panel zone.
4. The results of calculated strengths of each component fairly agreed with the test results, indicating that the calculation method can evaluate the capacity of the exterior beam-column joints.

REFERENCES

- [1] H. Kuramoto and Fauzan, "Feasibility Study on Engineering Wood Encased Concrete-Steel Composite Columns, Proceedings of Eleventh International Colloquium on Structural and Geotechnical Engineering (11thICSGE), Ain Shams University, Cairo, Egypt, CD-ROM Paper Code-F05ST20, May 2005.
- [2] Fauzan, Kuramoto, H. and Kim, K-H., "Seismic Performance of Composite EWECs Columns using Single H-steel," Proceedings of JCI, Vol.27, No.2, pp.307-312, June 2005.
- [3] Fauzan, Kuramoto, H., Matsui, T. and Kim, K-H., "Seismic Behavior of Composite EWECs Columns with Varying Shear-Span Ratios", Proceedings of JCI, Vol. 28, No.2, pp.1357-1362, July 2006.
- [4] Fauzan, Kuramoto, H. and Matsui, T., "Seismic Behavior of Interior Beam-Column Joints for Composite EWECs Structural Systems, Journal of Structural Engineering, Vol.53B, pp.389-396, April 2007.
- [5] Architectural Institute of Japan, AIJ Standard for Structural Calculation of Steel Reinforced Concrete Structures", Tokyo, 2001.